Electronic Supplementary Material (ESI) for Nanoscale.

Supporting Information

One-pot stirring-free Synthesis of silver nanowires with tunable lengths and diameters via Fe^{3+} & Cl^- co-mediated polyol method and their application as transparent conductive films

Kan Zhan, Rui Su, Sihang Bai, Zhenhua Yu, Nian Cheng, Changlei Wang, Sheng Xu, Wei Liu, Shishang Guo*, Xing-Zhong Zhao**

School of Physics and Technology, Key Laboratory of Artificial Micro/Nano Structures of Ministry of Education, Wuhan University, Wuhan, 430072, China

*Corresponding authors. Tel:+86-27-8764 2784. Fax:+86-27-6875 2569.

E-mail: xzzhao@whu.edu.cn (X.Z.), gssyhx@whu.edu.cn (S.G.), wliu@whu.edu.cn (W.L.)

Table of Contents

More details of the experimental section

Materials

Inorganic salts, including ferric chloride hexahydrate ($FeCl_3 \cdot 6H_2O$, 99.0%), potassium chloride (KCl, 99.5%), ferric nitrate nonahydrate ($Fe(NO_3)_3 \cdot 9H_2O$, 98.5%), as well as solvents, like ethylene glycol (EG, ≥ 99.0%), ethanol (99.7%), acetone (99.5%) were all purchased from Sinopharm Chemical Reagent Co., Ltd. Silver nitrate (AgNO3, 99.8%) powder was obtained from Shanghai Lingfeng Chemical Reagent Co., Ltd, and poly(vinyl pyrrolidone) (PVP, Mw ≈ 55,000) was purchased from Sigma-Aldrich Corporation. All chemicals were of analytic grade (AR) and were used as received without further purification.

Fabrication of transparent conductive films

To fabricate pristine TCFs composed of AgNWs, the original AgNWs products were cleaned to obtain inks of them. A selected resultant was firstly diluted (8 times by volume) in the mixture of ethanol and acetone and underwent successive centrifugation at 3000 rpm for 15 min to purify it. After each centrifugation, the supernatant was removed and the precipitate was redispersed in mixed solution of ethanol and acetone for next clean procedure. The cleaning process was repeated for three times. Then, the cleaned product was dispersed in ethanol and stored for future use.

After the finish of Ag NW ink preparation, the silver nanowire films were fabricated using a KW-4A spin-coating apparatus. To gain Ag NW films with various coverages, so as to attain a series of transparency and sheet resistance, suspensions of Ag NW dispersed in ethanol with different concentrations were used and varied times of spin coating were carried out. It should be noted that each subsequent coating was conducted after previous one was dried on a hotplate (60 ℃) in air, beneficial for uniform coating.

Characterization

In order to observe the morphology of samples prepared from different recipes, scanning electron microscopy (SEM) was performed either on FE-SEM of Sirion (200) equipped with an EDS detector, or on FE-SEM of Hitachi (S-4800). The samples of SEM were cleaned to remove insulating PVP under an high centrifugation speed of 8000 rpm, ensuring complete retention of all products. Optical images were recorded under the dark mode of a metalloscope (BX51M, Olympus). The UV-vis spectra were measured on Perkinelmer LAMBDA 650 UV/Vis Spectrophotometer. For solution samples, a pair of quartz cells with 1 cm optical path was used, and several drops of the original solution products were diluted by ethanol in the container. In all cases, a blank sample was put on the reference side to deduct the effects of substrates. The X-ray diffraction (XRD) patterns were recorded on a Bruker-AXS D8 Focus diffractometer with Cu Kα radiation (λ = 1.54056 Å), and samples of thick AgNWs films on nylon filter membranes (0.45 μm, 60 mm) were prepared by vacuum filtration of AgNWs solution to do the test. To measure the Rs of AgNWs films, two strips of electrical contact pads were prepared at the both ends of each sample by using indium soldering, and the resistances were measured by a multimeter (UNI-T, UT30B). The Rs could be calculated using the equation of Rs = R(W/L), where W and L were the width and length of the tested rectangular films, respectively.

Table S1. A list of synthetic conditions and statistical results of different reactions[a]

Section	Trail names	Amount of standard solution (mL)			Sizes D (nm); L (μm)	Aspect ratio (AR=L/D)	NWs yield (%)	Remarks
		KCl	$Fe(NO_3)_3$	$FeCl_3$				
3.1.1.1	$FeCl_3$-STD	0	0	0.4	94.5;38.0	402	97.3	--
3.1.1.2	NONE	0	0	0	--	--	0	only NPs
	Cl^- only	0.4	0	0	61.3;15.6	255	> 95	--
	Fe^{3+} only	0	0.4	0	--	--	< 20%	non-uniform NWs
	Fe^{3+}&Cl^-	0.4	0.4	0	93.7;38.5	411	> 95	equal to $FeCl_3$-STD
3.1.2	KCl control	0.1~10	0	0	45~77; 11~18	235~270	> 90	--
3.1.3	$FeCl_3$ control	0	0	0.1~1.0	77~221; 13~230	174~1423	> 90	--
				1.5~3.0	125~158; 92~147	730~927	< 80	NWs and irregular NPs
3.2.1.1	Fe4Cln	0.1~1.0	0.4	0	72~130; 26~38	280~402	> 95	--
3.2.1.2	FenCl4	0.4	0.1~1.0	0	61~200; 13~226	210~1618	> 90	--

[a] Note. All the trials were carried out under the same condition from standard reaction, except the difference in amount of added additives.

Fig. S1. OM and SEM images comparison of KCl reactions

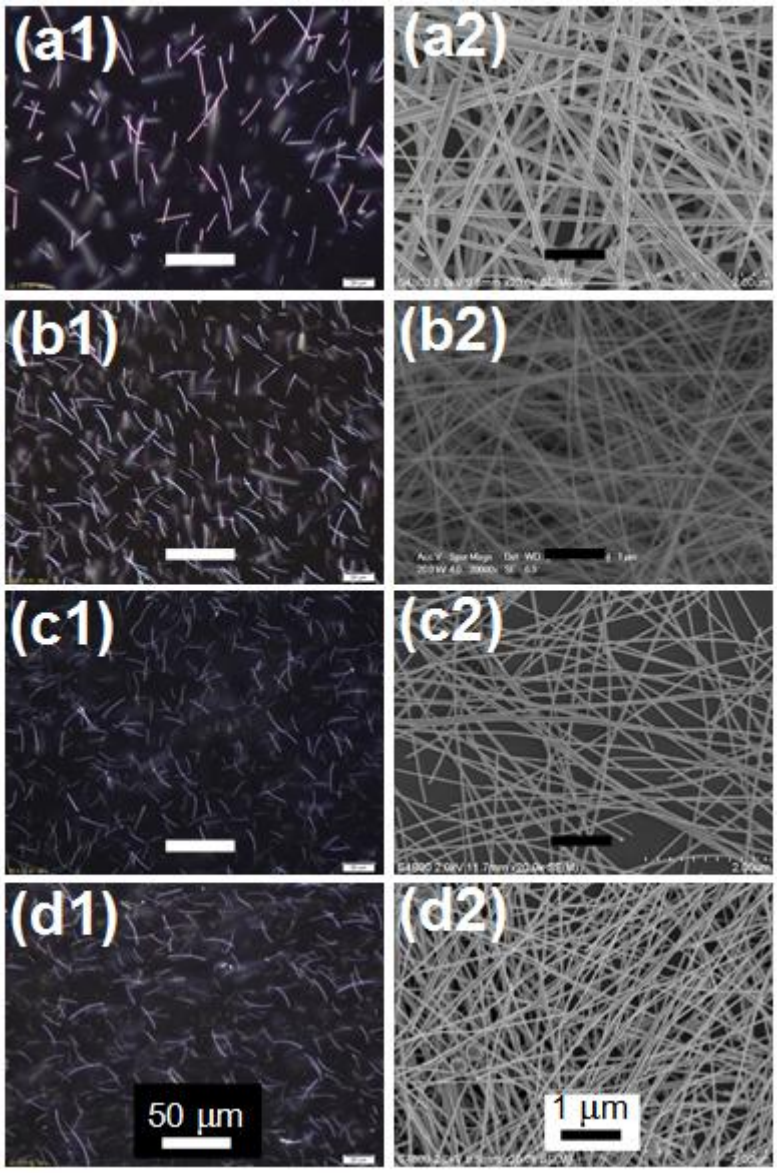

Fig. S1. Products comparison of reactions with different addition amounts of KCl. The amount of added KCl solution is (a1,a2) 0.1 mL, (b1,b2) 0.7 mL, (c1,c2) 1.5 mL, and (d1,d2) 10 mL, respectively. For simplicity, images with other addition amounts are excluded. The scale bars are all 1 µm in SEM images and all 50 µm in optical images.

Fig. S2. SEM image of precipitates from 3mL $FeCl_3$ and their EDS spectrum

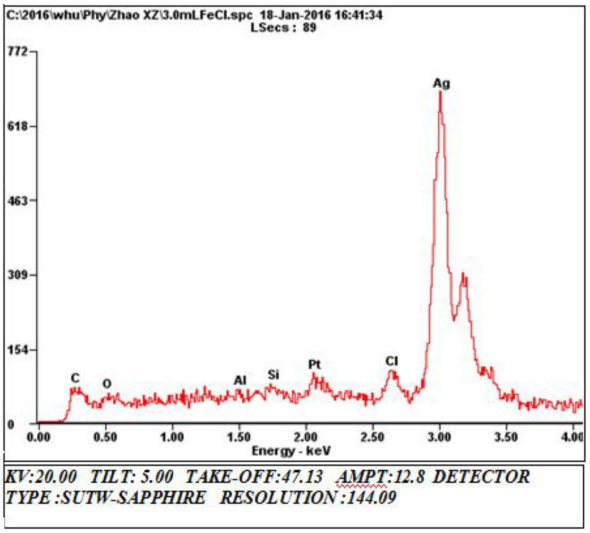

Element	Wt %	At %
PtM	07.13	03.95
ClK	01.48	04.52
AgL	91.38	91.53

EDAX ZAF QUANTIFICATION STANDARDLESS SEC
TABLE : DEFAULT

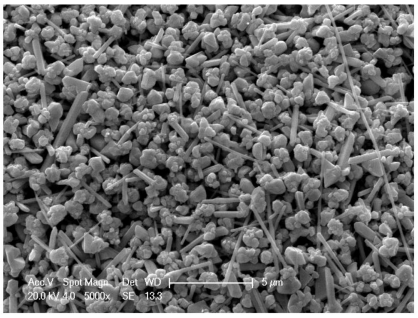

Figure S2. SEM image of precipitates from 3mL $FeCl_3$ and their EDS spectrum. The existence of AgCl composition is verified from the EDS spectrum, where the peak of Cl atom is evident. The nanoparticles in SEM image present irregular shapes, accompanied by a few silver nanorods.

Fig. S3. Digital images recording the color variations during the reaction of $FeCl_3$-STD

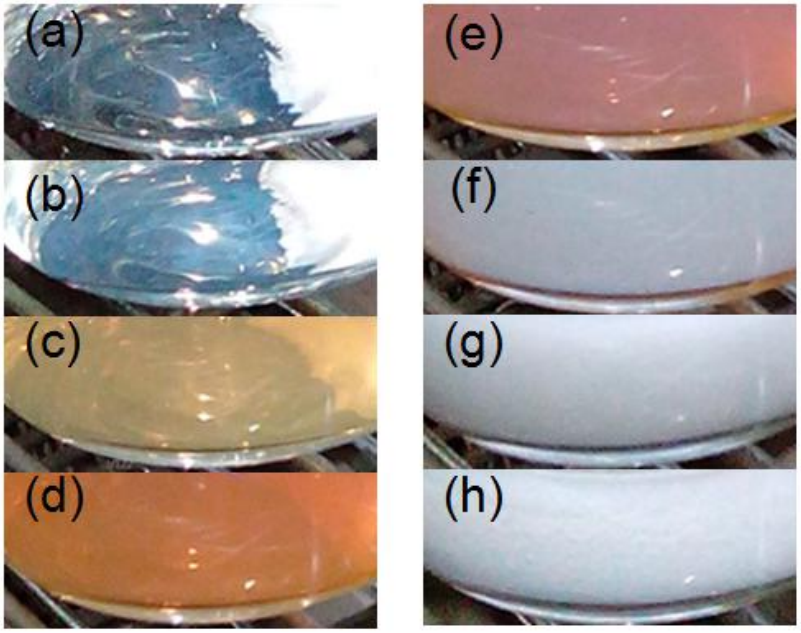

Figure S3. Digital images recording the color variations during the reaction of $FeCl_3$-STD. The recorded time were t = (a) 0 min, (b) 5 min, (c) 15 min, (d) 30 min, (e) 45 min, (f) 1 hr 15 min, (g) 2 hrs, and (h) t = 4.5 hrs at last, respectively.

Fig. S4 AgCl NPs in sample taken from the bottom of the flask after the reaction completed

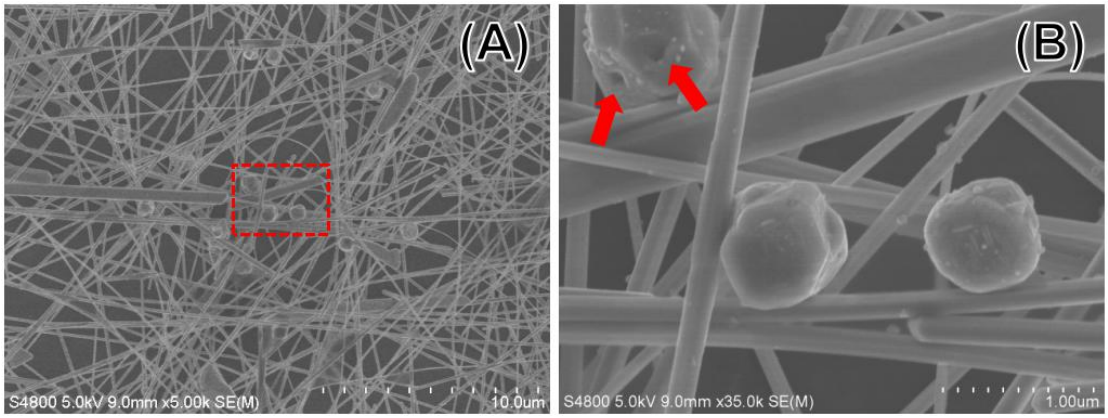

Figure S4. AgCl NPs in sample taken from the bottom of the flask after the reaction completed. There were some AgCl NPs existing in Fig. S4(A), and their distribution is quite sparse due to small amount after reaction. Moreover, a magnified picture in Fig. S4(B) illustrates that there are some hollow points on the surface of AgCl NPs, indicating that some silver nanostructures have separated from them after sufficient growth. These pictures further proves the advantage of our reaction process to gain AgNWs with high purity.

Fig. S5. OM and SEM images comparison of Fe4Cln reactions

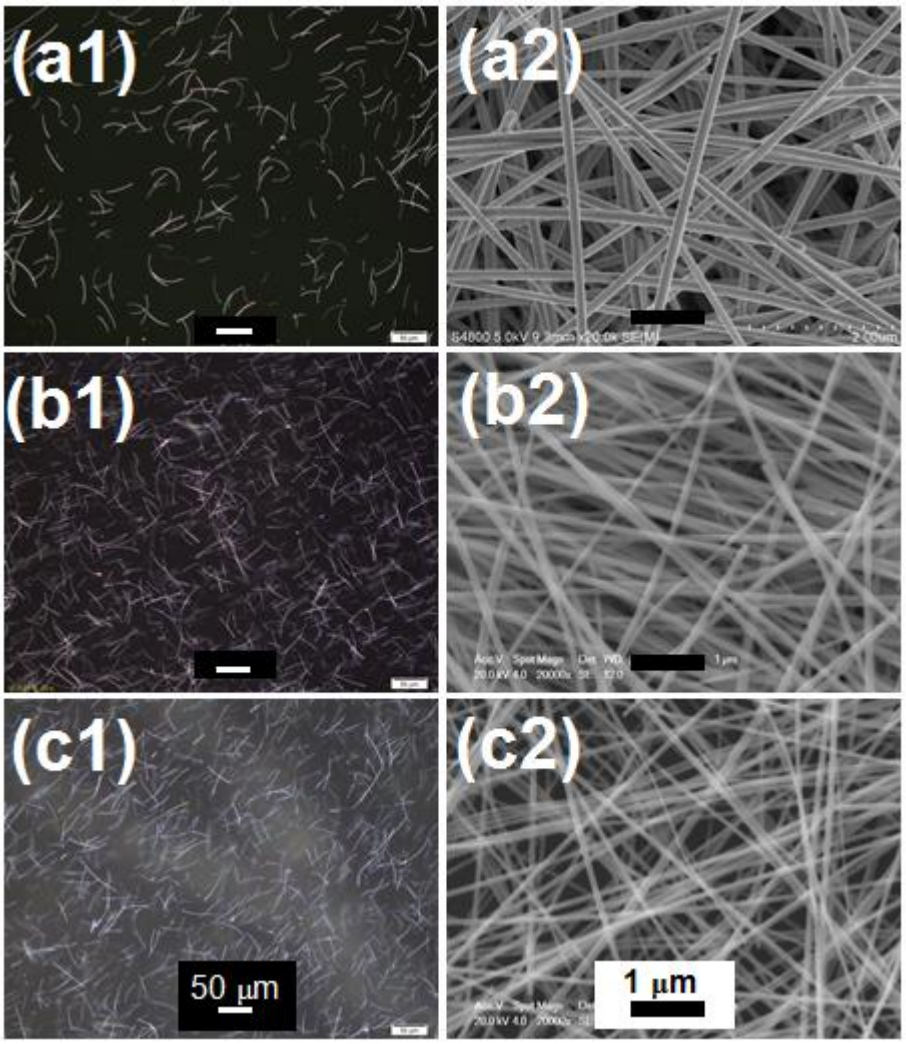

Figure S5. Products comparison of Fe4Cln reactions. The amount of Cl^- was changed by injection of KCl solution with different volumes of (a1,a2) 0.1 mL, (b1,b2) 0.7 mL, and (c1,c2) 1.0 mL, respectively, while the amount of Fe^{3+} is fixed by addition of 0.4 mL $Fe(NO_3)_3$ solution. For simplicity, images with other addition amounts are excluded. The scale bars are all 1 μm in SEM images and all 50 μm in optical images.

Fig. S6. OM and SEM images comparison of FenCl4 reactions

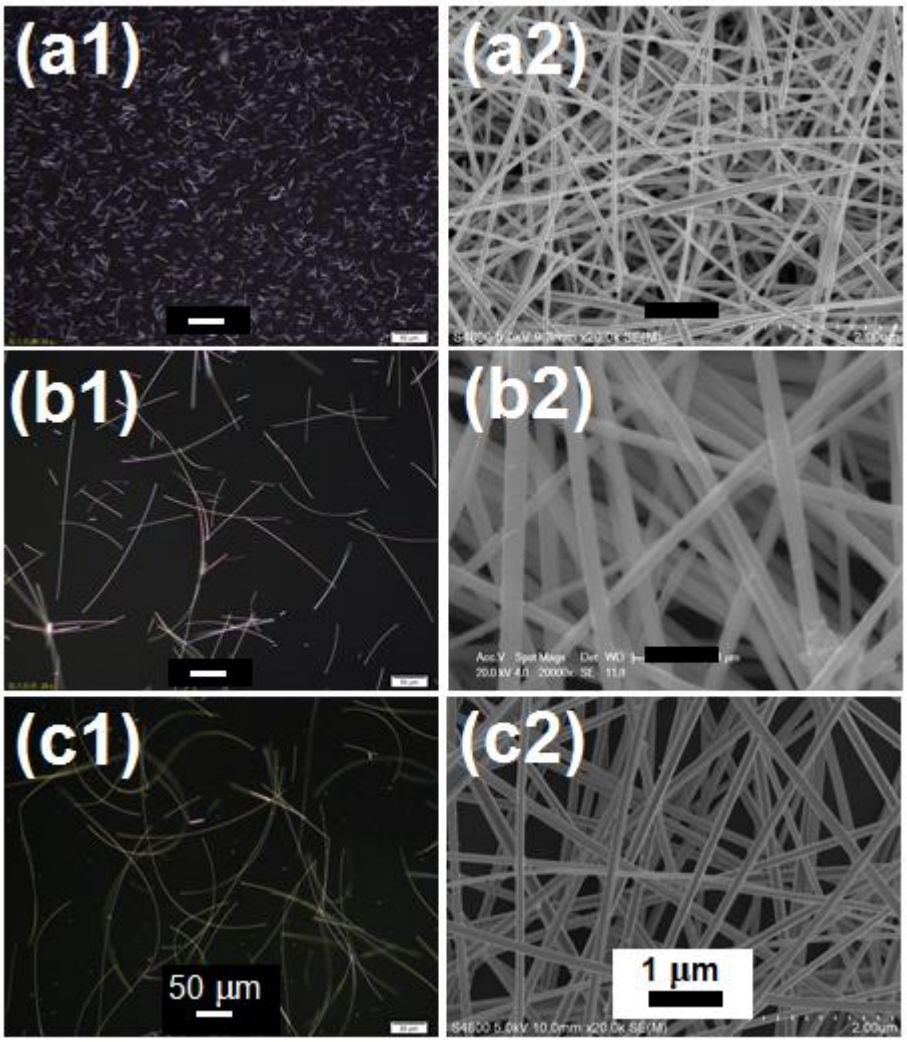

Figure S6. Products comparison of FenCl4 reactions. The amount of Fe^{3+} was changed by injection of $Fe(NO_3)_3$ solution with different volumes of (a1,a2) 0.1 mL, (b1,b2) 0.7 mL, and (c1,c2) 1.0 mL, respectively, while the amount of Cl^- is fixed by addition of 0.4 mL KCl solution. The scale bars are all 1 μm in SEM images and all 50 μm in optical images.

Fig. S7. XRD patterns of powder samples

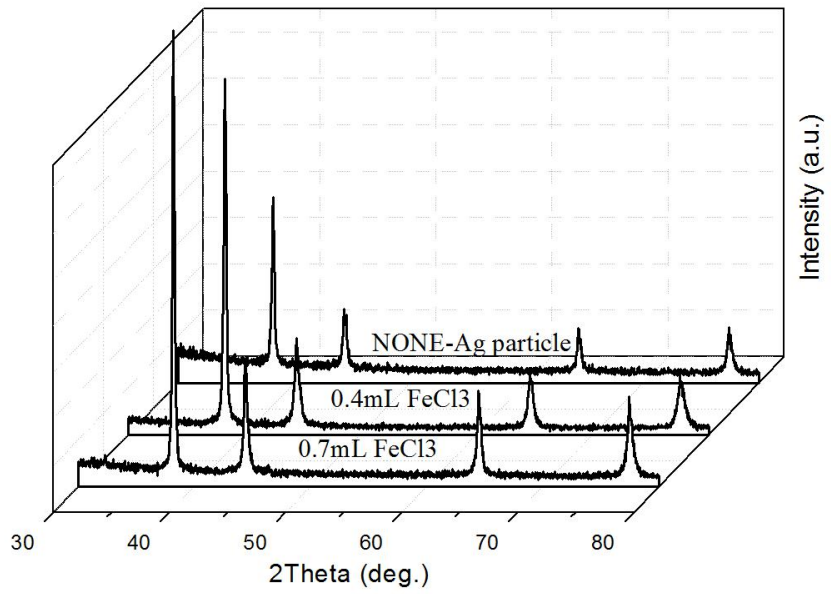

Figure S7. XRD patterns of powder samples. The weak peaks from (220) and (311) in XRD patterns of film samples became evident when powder samples were employed to do the tests.

Table S2. Peak parameters extracted from XRD patterns of powder samples and films with different thicknesses.

Sample name	lattice constant (Å)	FWHM index (degree)			Intensity ratio of (111)/(200)		
		sample status			sample status		
		thin film	thick film	powder	thin film	thick film	powder
3mL KCl	4.0599	0.297	0.366	--	4.04	2.07	--
0.4mL FeCl3	4.0496	0.075	0.156	0.228	8.1	6.93	3.99
0.7mL FeCl3	4.0773	0.084	0.103	0.203	5.49	5.06	3.95
Ag particles (NONE)	4.0843	0.190	--	0.244	3.31	--	2.71
Bulk Ag	4.0862	N/A			2.50		

Fig. S8. Optical images showing the agglomeration points in Fe10Cl4 film

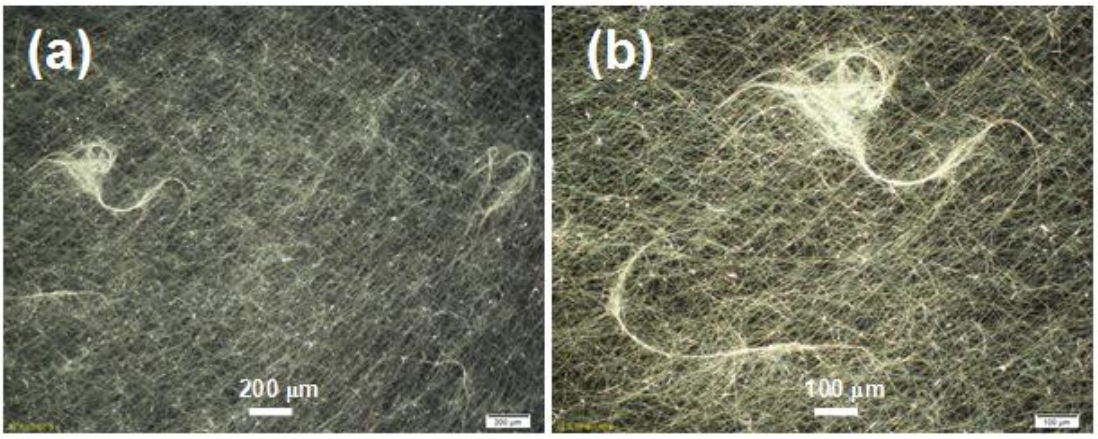

Figure S8. Optical images showing the agglomeration points in Fe10Cl4 film.

Fig. S9. Optical images for comparison of wire density under same transparency in pristine AgNW films with different NW sizes

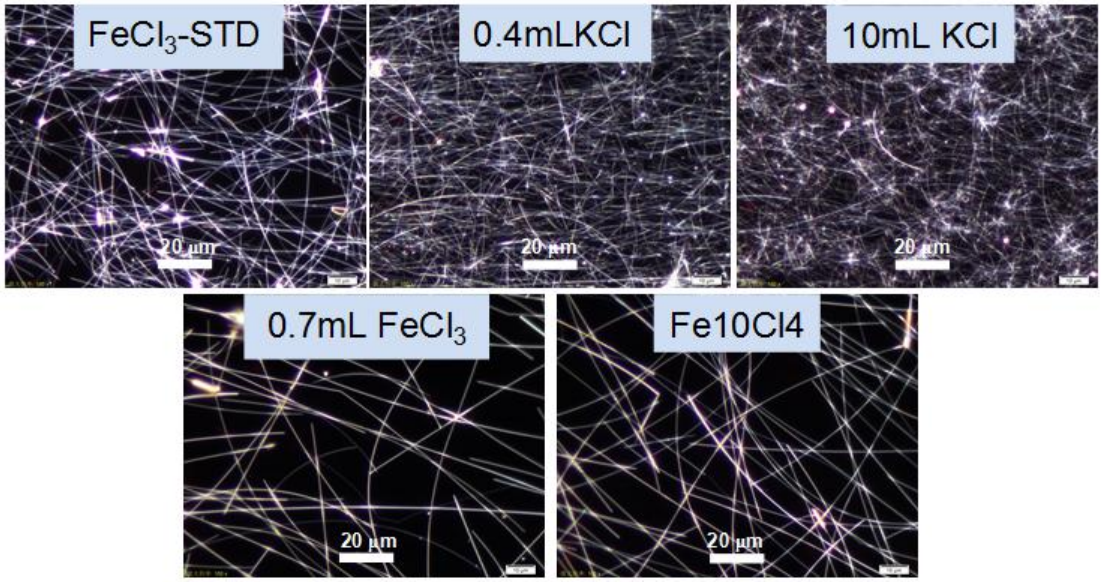

Figure S9. Optical images for comparison of wire density under same transparency in pristine AgNW films with different NW sizes. The transparency of all selected samples are close to 90%. The wire density in the film from small NWs of 10mL KCl is much larger than that of large wires from 0.7mL $FeCl_3$ and Fe10Cl4.